Stem Cell Reports
Article
ISSCR
OPEN ACCESS

# Hedgehog Activation Regulates Human Osteoblastogenesis

Shoko Onodera,[1,2] Akiko Saito,[1] Hironori Hojo,[2,3] Takashi Nakamura,[1] Denise Zujur,[2] Katsuhito Watanabe,[4] Nana Morita,[5] Daigo Hasegawa,[4] Hideki Masaki,[6] Hiromitsu Nakauchi,[6,7] Takeshi Nomura,[5] Takahiko Shibahara,[4] Akira Yamaguchi,[8] Ung-il Chung,[2,3] Toshifumi Azuma,[1,8,*] and Shinsuke Ohba[2,3,9,*]
[1]Department of Biochemistry, Tokyo Dental College, Tokyo 101-0061, Japan
[2]Center for Disease Biology and Integrative Medicine, Graduate School of Medicine, The University of Tokyo, Tokyo 113-8656, Japan
[3]Department of Bioengineering, Graduate School of Engineering, The University of Tokyo, Tokyo 113-8655, Japan
[4]Department of Oral and Maxillofacial Surgery, Tokyo Dental College, Tokyo 101-0061, Japan
[5]Department of Oral Medicine, Oral and Maxillofacial Surgery, Tokyo Dental College, Chiba 272-8513, Japan
[6]Center for Stem Cell Biology and Regenerative Medicine, Institute of Medical Science, The University of Tokyo, Tokyo 108-8639, Japan
[7]Institute for Stem Cell Biology and Regenerative Medicine, Stanford University School of Medicine, Stanford, CA 94305-5461, USA
[8]Oral Health Science Center, Tokyo Dental College, Tokyo 101-0061, Japan
[9]Department of Cell Biology, Graduate School of Biomedical Sciences, Nagasaki University, Nagasaki 852-8521, Japan
*Correspondence: tazuma@tdc.ac.jp (T.A.), s-ohba@nagasaki-u.ac.jp (S.O.)
https://doi.org/10.1016/j.stemcr.2020.05.008

## SUMMARY

Two genetic diseases, Gorlin syndrome and McCune-Albright syndrome (MAS), show completely opposite symptoms in terms of bone mineral density and hedgehog (Hh) activity. In this study, we utilized human induced pluripotent stem cell (iPSC)-based models of the two diseases to understand the roles of Hh signaling in osteogenesis. Gorlin syndrome-derived iPSCs showed increased osteoblastogenesis and mineralization with Hh signaling activation and upregulation of a set of transcription factors in an osteogenic culture, compared with the isogenic control. MAS-specific iPSCs showed poor mineralization with low Hh signaling activity in the osteogenic culture; impaired osteoblastogenesis was restored to the normal level by treatment with an Hh signaling-activating small molecule. These data suggest that Hh signaling is a key controller for differentiation of osteoblasts from precursors. This study may pave a path to new drug therapies for genetic abnormalities in calcification caused by dysregulation of Hh signaling.

## INTRODUCTION

Hedgehog (Hh) signaling is a highly conserved pathway between species, acting as a mitogen and morphogen in various developmental processes (Ingham and McMahon, 2001). Mouse genetics studies have highlighted the requirement of Hh signaling to specify skeletal progenitors into osteoblast precursors expressing runt-related transcription factor (TF) 2 (Runx2), a master TF for osteoblast development (Komori et al., 1997; Long et al., 2004). Both Gli activators and repressors affect the Hh function in this context (Joeng and Long, 2009). In adult mice, constitutive activation of Hh signaling by *Patched1* (*Ptch1*) haploinsufficiency led to high bone mass with an acceleration of both bone formation and bone resorption (Ohba et al., 2008).

Dysregulation of Hh signaling has been implicated in human diseases (Mullor et al., 2002). Mutations of *PTCH1*, which encodes a receptor of Hh, are known to cause Gorlin syndrome (OMIM 109400), a rare autosomal-dominant disorder characterized by multiple tumor formation and skeletal anomalies (Gorlin, 1995; Gorlin and Goltz, 1960). Most individuals with this disease have skeletal anomalies, and ectopic calcification particularly in the cerebral falx is present in more than 90% of the affected individuals. Heterozygous *Ptch1*-deficient ($Ptch1^{+/-}$) mice have features that recapitulate those of patients with Gorlin syndrome (Goodrich et al., 1997). They have higher bone mineral density than age-matched controls (Ohba et al., 2008).

Molecular mechanisms underlying the maintenance of human bone mass have attracted much attention due to their fundamental importance for the understanding of bone pathology. From this point of view, it is noteworthy that two different Hh-related syndromes, Gorlin syndrome and McCune-Albright syndrome (MAS) (OMIM 174800), are characterized by completely opposite features of osteoblast differentiation. Gorlin syndrome exhibits activation of Hh signaling and enhancement of mineralization, while MAS is often accompanied with fibrous dysplasia (FD) of immature bones with poor mineralization (Albright et al., 1937; Weinstein et al., 1991). FD is a genetic, non-inheritable rare bone disease caused by a postzygotic mosaic activation mutation (*R201H* or *R*201C) of the α-subunit of stimulatory G protein (Gαs) encoded by GNAS, and this mutation is also observed in MAS (Albright et al., 1937; Lichtenstein, 1938; Turan and Bastepe, 2015). FD often leads to wheelchair life due to bone deformation, fractures, and severe pain. Khan et al. (2018) elegantly described that a Gnas (R201H) knockin mouse line showed reduced mineralization in the mutant bones, and the increased osteoid surface demonstrated poor osteoblastogenesis with suppressed Hh signaling and enhanced Wnt signaling.

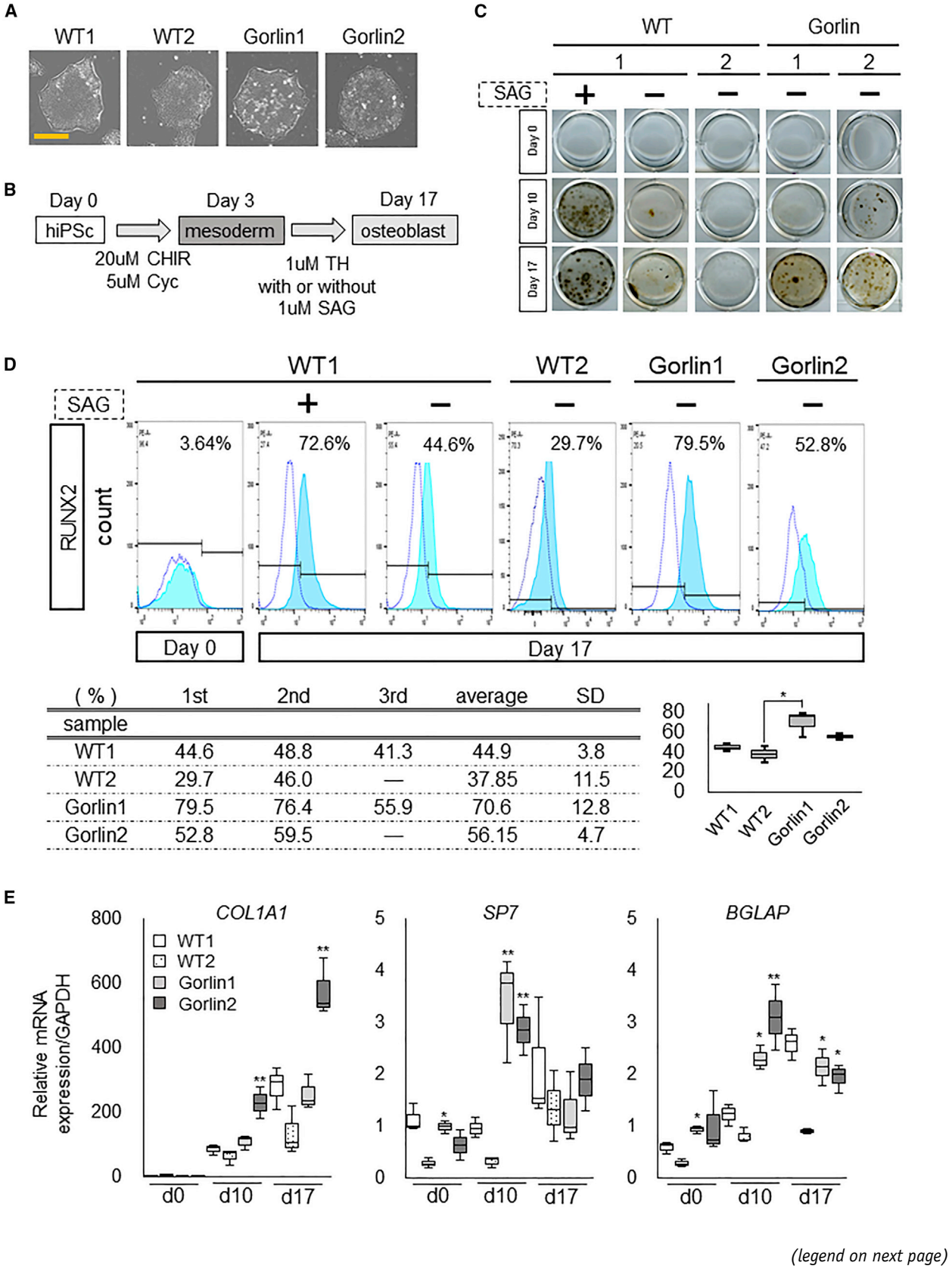


*(legend on next page)*

Despite the opposite status of Hh signaling and osteogenesis in the two Hh-related genetic diseases, few studies have focused on differences in the mechanisms of bone formation, particularly the mechanisms involving osteoblast differentiation, between the diseases. In addition, although human cell models of these diseases would help elucidate their pathogenesis at the cellular and molecular levels and help develop therapeutic strategies, such models remain to be established.

We previously generated induced pluripotent stem cells (iPSCs) derived from patients with Gorlin syndrome (Gorlin iPSCs), who therefore carried heterozygous loss-of-function mutations in *PTCH1*; Gorlin iPSCs showed hypersensitivity to Hh signaling, and Hh signaling may be associated with accelerated osteoblast differentiation (Hasegawa et al., 2017). Gorlin iPSCs also demonstrated enhanced Hh signaling, which in turn suppressed Wnt and BMP signaling (Hasegawa et al., 2017). However, once cultured in a conventional osteogenic differentiation medium, they suddenly acquired steep upregulation of Wnts and BMPs to promote osteoblastogenesis. Therefore, it was necessary to investigate the process of osteoblast differentiation of Gorlin iPSCs in defined culture systems, to examine the direct effect of Hh activation on human osteoblast differentiation. In addition, we generated MAS-specific iPSCs (MAS iPSCs) by introducing *GNAS* gene mutation with genome-editing techniques. MAS iPSCs had constitutively activated *GNAS*, which increased the cellular cAMP level under an unstimulated condition (T.A., S.O., K.W., A.S., T.S. and T.N., unpublished data). We reasoned that we would achieve a better understanding of the correlation between intracellular Hh signaling activity and osteogenic capacities by utilizing the two disease-specific iPSC lines.

In this study, we sought to gain insight into the involvement of Hh signaling in human osteoblastogenesis by taking advantage of the two platforms that we developed: the osteoblast induction protocol for human iPSCs, in which small-molecule-mediated activation of Hh signaling contributed to differentiation of human iPSCs (Kanke et al., 2014; Zujur et al., 2017), and the human iPSC-based disease models, Gorlin iPSCs and MAS iPSCs. This study provides a valuable foundation for establishing stem cell-based systems to delineate the mechanism of skeletal abnormalities underlying human genetic disorders. In addition, our results suggest the possibility of drug therapies for FD.

## RESULTS

### Osteogenic Capacities of Gorlin iPSCs in an Osteoblast Induction Culture

We previously established two iPSC lines from different patients with Gorlin syndrome (Gorlin iPSCs; see Experimental Procedures) (Hasegawa et al., 2017). We used Sanger sequencing to confirm that the *PTCH1*-loci mutations in each of the two Gorlin iPSC lines were the same as those identified in the tissues of the patients of origin (Figure S1A). Two other hiPSC lines that were not relevant to Gorlin syndrome were also prepared as controls (wild-type [WT] iPSCs; see Experimental Procedures). All four iPSC lines were adapted to a feeder-free condition in Essential 8 medium (see Experimental Procedures). We confirmed that the morphology of the Gorlin iPSC colonies was similar to that of the WT iPSC colonies under the conditions used; both the WT and Gorlin cells demonstrated tightly packed colonies of small cells with defined borders and the high nucleoplasmic ratio (Figure 1A). Both the WT and Gorlin iPSCs expressed markers of pluripotency, including *NANOG* and *SSEA4* (Figure S1B).

To elucidate the impact of Gorlin syndrome-associated *PTCH1* mutations on human osteoblastogenesis, we

**Figure 1. Osteogenic Capacities of Gorlin iPSCs in the Osteoblast Induction Culture**

(A) The morphology of colonies of WT and Gorlin iPSCs adapted to Essential 8 medium. Data of two lines (1 and 2) are shown for each type of iPSC. Scale bar, 100 μm.

(B) A schematic of the protocol of the osteoblast induction culture.

(C) Calcification in the osteoblast induction culture of WT and Gorlin iPSCs with or without SAG treatment. von Kossa staining was performed at days 0, 10, and 17 of the culture. Mineral deposition was detected as black staining. Data of two lines (1 and 2) are shown for each type of iPSC.

(D) Quantification of RUNX2-positive cells in the osteoblast induction culture of WT and mutant (MT) iPSCs by flow cytometry (FCM). The cells were cultured under a condition with or without SAG as indicated. FCM analysis was performed for RUNX2 at days 0 and 17 of the culture. Blue dotted lines show signal intensities from staining with the immunoglobulin G (IgG) isotype control. Light blue lines show signal intensities from the staining with an anti-RUNX2 antibody. The positive gate was set to the area where the isotype control was present at around 8%. The FCM analyses were performed in two or three independent experiments using two lines (1 and 2) for each type of iPSC; a representative histogram is shown.

(E) The mRNA expression of osteoblast marker genes in the osteoblast induction culture of WT and MT iPSCs without SAG. qRT-PCR analysis was performed at the indicated days of the cultures. Data are the means ± SD from three independent experiments using two lines (1 and 2) for each type of iPSC. *$p < 0.05$ versus WT2 iPSCs at the indicated day of the culture. **$p < 0.05$ versus both WT1 and WT2 iPSCs at the indicated day of the culture.

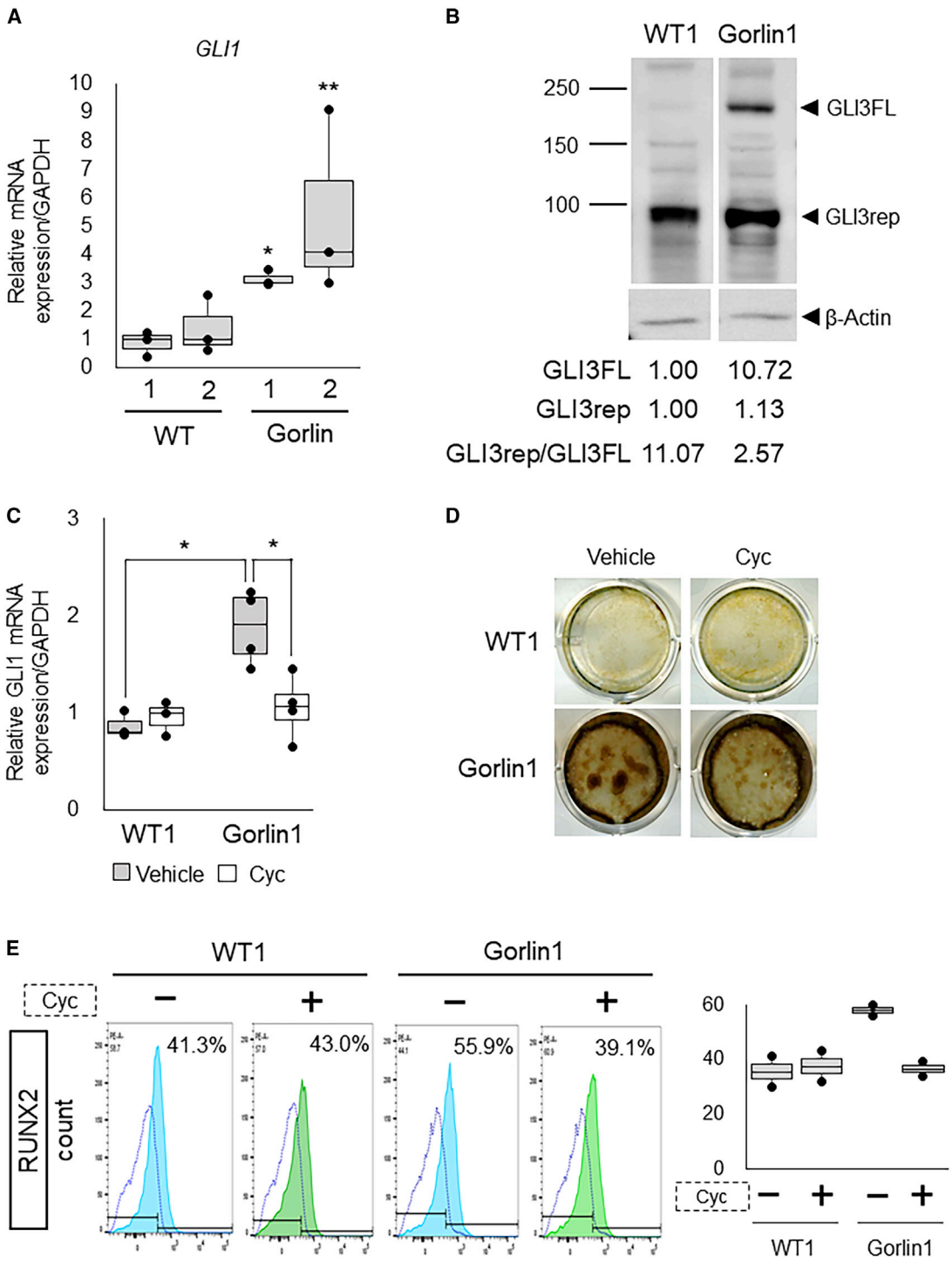


**Figure 2. Expression of GLI in the Gorlin iPSC-Derived Osteogenic Population**

(A) The mRNA expression of *GLI1* in the osteoblast induction culture of WT and MT iPSCs without SAG. qRT-PCR analysis was performed at day 17 of the culture. Data are the means ± SD from three independent experiments using two lines (1 and 2) for each type of iPSC. *$p < 0.05$ versus WT1 iPSCs. **$p < 0.05$ versus both WT1 and WT2 iPSCs. The normalized expressions are shown relative to those of calibrator samples (WT1 iPSCs on day 17).

(B) Protein expression of endogenous GLI3 in the osteoblast induction culture of WT1 and Gorlin-1 iPSCs. The GLI3 expression was analyzed by immunoblotting using specific antibodies at day 17 of the culture. Band intensities were quantified by normalization to those

*(legend continued on next page)*

cultured Gorlin and WT iPSCs according to our stepwise osteoblast differentiation protocol, in which 3-day mesoderm induction is followed by 14-day osteoblast induction (Kanke et al., 2014) (Figure 1B). In that protocol, the osteogenic molecule TH (Ohba et al., 2007) and the Smoothened agonist (SAG), which was an Hh signaling activator, are used in the osteoblast induction phase; we confirmed that the protocol achieved the activation of Hh signaling and upregulation of osteoblast marker genes in WT iPSCs by the 17th day of culture (Figure S2). These results suggest that the osteoblast induction is at least partly linked with Hh signaling activation in the protocol.

Both WT iPSCs and Gorlin iPSCs showed decreased expression of the pluripotency marker *POU5F1* and increased expression of the mesoderm marker *MIXL1* at the end of the mesoderm induction stage (day 3) compared with those at day 0; there was no clear difference in the expression of these genes between the genotypes (Figures S3A and S3B). To induce osteoblast differentiation of the WT iPSC- or Gorlin iPSC-derived mesodermal cells, we then treated them with TH in the presence or absence of SAG for another 2 weeks (Figure 1B). von Kossa staining at day 17 of the culture revealed that Gorlin iPSCs showed increased calcification compared with WT iPSCs even in the absence of SAG (Figure 1C; compare the right four rows). WT iPSCs with SAG treatment showed increases in calcification compared with those without SAG treatment (Figure 1C; compare the left two rows and Figure S3C). In addition, Gorlin iPSCs with SAG treatment showed increases in calcification compared with those without SAG treatment (Figure S3D). These data suggest that Hh signaling activation could enhance the calcification of osteoblasts derived from iPSCs.

To examine whether the increased calcification is related to the enhancement of osteoblast differentiation, we checked the expression of osteoblastic markers in the culture of each iPSC line. Since Hh input is required for the specification of progenitors into Runx2-positive osteoblast precursors (Long et al., 2004; St-Jacques et al., 1999), we analyzed RUNX2-positive cells by flow cytometry at day 17 of the culture. As shown in Figure 1D, Gorlin iPSC cultures showed a higher percentage of RUNX2-positive cells than WT iPSC cultures in the absence of SAG (Figure 1D). In addition, qRT-PCR analysis demonstrated that the expression level of *COL1A1*, an early marker of osteoblast differentiation, and the expression levels of *SP7* and *BGLAP*, mid- to late osteoblast markers, were significantly higher in Gorlin iPSCs than in WT iPSCs with no SAG treatment (Figure 1E). However, the difference was noticeable at day 10 and became less at day 17. This may represent accelerated differentiation of Gorlin iPSCs at the earlier phase of the culture, and WT iPSCs may reach the similar level to Gorlin iPSCs at the later phase. In addition, Gorlin iPSCs were unlikely to further differentiate or maturate at the later phase. Thus, the increased calcification of Gorlin iPSCs in the osteoblast induction culture was accompanied with higher expressions of osteoblast markers, supporting augmentation of the osteogenic capacity in Gorlin iPSCs even without exogenous activation of Hh signaling; Gorlin syndrome-associated *PTCH1* mutations are likely to have positive impacts on human osteoblastogenesis. The phenotypes of Gorlin iPSCs support our previous findings that patients with Gorlin syndrome and *Ptch1*$^{+/-}$ mice exhibited increases in bone mass with accelerated bone formation (Goodrich et al., 1997; Ohba et al., 2008).

## Changes of GLI TFs in Gorlin iPSCs upon the Osteoblast Induction

Since previous findings showed ectopic activation of Hh signaling in *Ptch1*$^{+/-}$ mice (Goodrich et al., 1997), we next explored whether downstream mediators of the signaling were affected in Gorlin iPSCs upon the osteoblast induction. The mRNA expression of *GLI1*, a readout of Hh signaling as well as a transcriptional activator acting downstream of the signaling (Ingham and McMahon, 2001), was significantly upregulated in Gorlin iPSCs compared with WT iPSCs in the osteoblast induction culture (Figure 2A). This result suggests that the Gorlin syndrome-associated *PTCH1* mutation leads to constitutive activation of Hh signaling in human osteoblastogenesis. This is consistent with the previous notion that heterozygous germline loss-of-function mutations of *PTCH1* release PTCH1-mediated SMO suppression and thereby activate Hh signaling (Alman, 2015; Briscoe and Thérond, 2013; Fujii and Miyashita, 2014).

of β-actin in each group. GLI3FL and GLI3rep indicate their relative intensity levels to WT1; GLI3rep/GLI3FL indicates the ratio of intensity levels of GLI3rep to those of GLI3FL in each group.

(C) The mRNA expression of *GLI1* in the osteoblast induction culture of WT1 and Gorlin-1 iPSCs with or without cyclopamine (Cyc). qRT-PCR analysis was performed at day 17 of the culture. Data are the means ± SD from three independent experiments. *$p < 0.05$. The normalized expressions are shown relative to those of WT1 iPSCs on day 17.

(D) Calcification in the osteoblast induction culture of WT1 and Gorlin-1 iPSCs with or without cyclopamine (Cyc). von Kossa staining was performed at day 17 of the culture.

(E) Quantification of RUNX2-positive cells in the osteoblast induction culture of WT1 and Gorlin-1 iPSCs without SAG, in the presence or absence Cyc. FCM analysis was performed for RUNX2 at day 17 of the culture. Blue dotted lines show signal intensities from the staining with the IgG isotype control. Light blue and green lines show signal intensities from the staining with an anti-RUNX2 antibody.

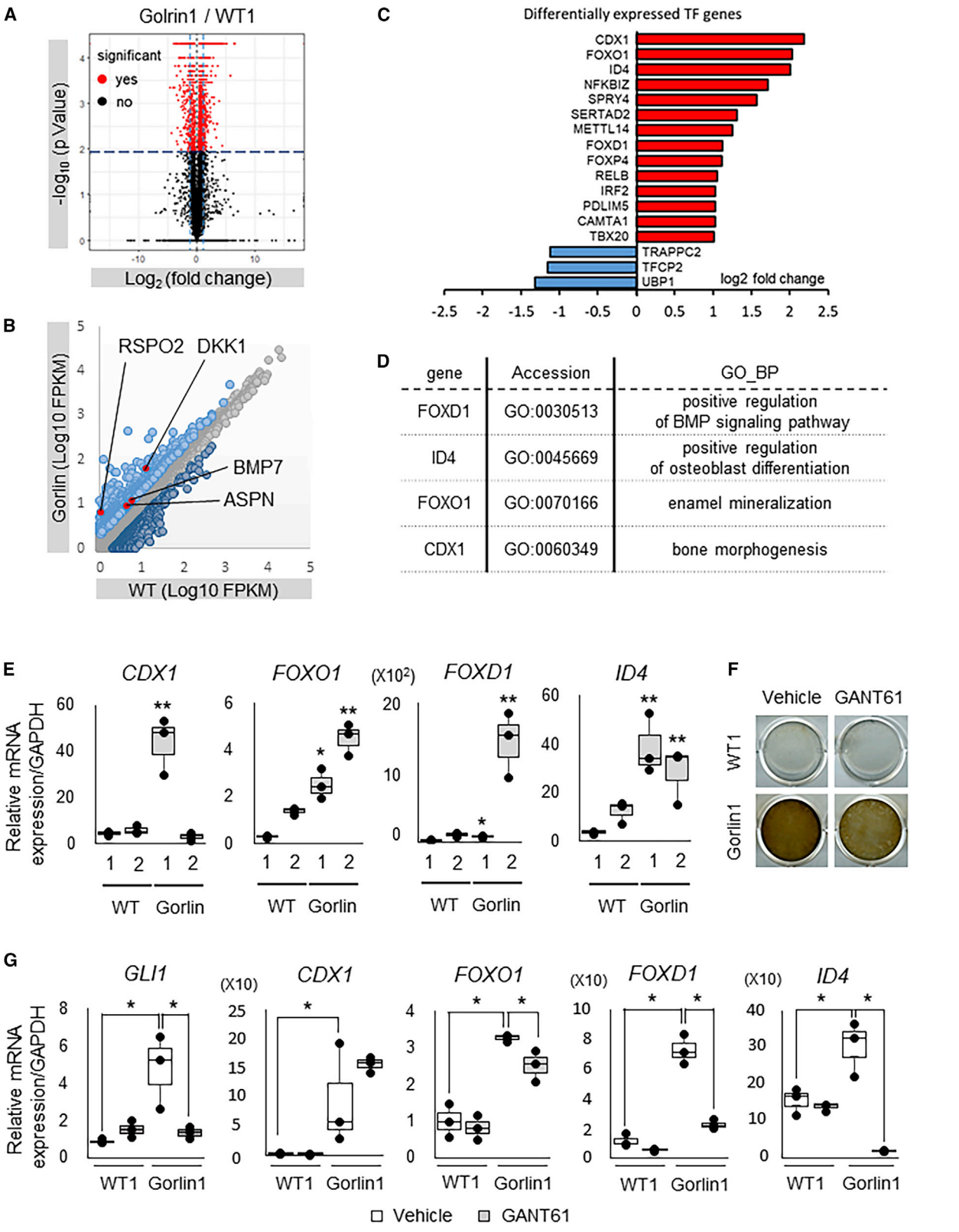


*(legend on next page)*

Hh signaling has also been demonstrated to regulate the expression of GLI3 as well as GLI1; the signaling suppresses processing of Gli3 into its truncated form in mouse limb bud cells (Wang et al., 2000), and mouse genetics and biochemical studies support the idea that Gli3 exerts repressive actions on osteoblast differentiation (Ohba et al., 2008). Based on these reports, we investigated the protein expression of GLI3 in WT and Gorlin iPSCs. The truncated repressor form of GLI3 (GLI3rep) was detected in both WT and Gorlin iPSCs at a similar level (Figure 2B). Although the full-length form of GLI3 (GLI3FL) was the minor form in both WT and Gorlin iPSCs, the amount of GLI3FL was much increased in Gorlin iPSCs (Figure 2B). As a result, the ratio of GLI3rep to GLI3FL was decreased in Gorlin iPSCs compared with WT iPSCs. These data suggest that GLI3 processing is suppressed by the Gorlin syndrome-associated *PTCH1* mutation in human osteoblastogenesis, probably due to the activation of Hh signaling demonstrated by *GLI1* upregulation (Figure 2A).

To clarify the involvement of Hh signaling activation in the augmented osteogenic capacity of Gorlin iPSCs, we investigated the effect of Hh inhibition on osteoblast differentiation by cyclopamine, an Smo antagonist that suppresses the Hh signaling activity. Treatment with cyclopamine resulted in neither an increase in *GLI1* expression nor an enhancement of calcification in Gorlin iPSCs at day 17 of the osteoblast induction culture (Figures 2C and 2D). Treatment with cyclopamine alone did not cause any change in *GLI1* expression or calcification in WT iPSCs at day 17 (Figures 2C and 2D). We also examined the percentage of RUNX2-positive cells in WT and Gorlin iPSCs with or without the cyclopamine treatment. Consistent with the above results, cyclopamine treatment reduced the ratio of Runx2-positive cells only in Gorlin iPSCs (from 55.9% to 39.1%) (Figure 2E). Thus, these data suggest that Hh signaling activation plays an important role in the enhancement of osteoblastogenesis and mineralization in Gorlin iPSCs.

## Expression Profiling of Gorlin iPSCs in the Osteoblast Induction Culture

To examine which signaling pathways and genetic networks were affected by Gorlin syndrome-associated *PTCH1* mutation in human osteoblastogenesis, we performed RNA sequencing (RNA-seq) analysis in the osteoblast induction culture (without SAG treatment) of WT and Gorlin iPSCs (Gorlin 1). The triplicate samples of each genotype were clustered in the same group (Figure S4A), and the average expression values of the triplicate were used for further analysis. We identified 753 genes that were differentially expressed between the Gorlin iPSC- and WT iPSC-derived osteoblastic populations at day 17 of the culture, according to the criteria shown in Figure S4B; 559 genes were upregulated and 194 genes were downregulated in Gorlin iPSCs compared with WT iPSCs (Figures 3A and 3B; Table S1). Genes related to osteoblast differentiation and calcification, such as *ASPN*, *BMP7*, *RSPO2*, and *DKK1*, were included as the differentially expressed genes (Figure 3B). A pathway enrichment analysis using DAVID identified multiple gene ontology (GO) categories that were significantly enriched in the differentially expressed genes (Table S2). It is notable that the enriched GO terms derived from the 193 downregulated genes were related to the cell cycle, including nuclear division (GO:0000280), mitosis (GO:0007067), and the M phase of the mitotic cell cycle (GO:00000087). This result may reflect acceleration of

**Figure 3. Transcriptome Analyses in the Gorlin iPSC-Derived Osteogenic Population**

(A) The volcano plot of gene expression between WT1 and Golrin-1 cells differentiated from iPSCs in RNA-seq analysis. Statistical significance genes that were calculated by Cuffdiff with red dots. Dark blue line and light blue line were the criteria indicated in Figure S4B.

(B) Scatterplot indicating the ratio of gene expressions between WT1 and Gorlin-1 cells differentiated from iPSCs in RNA-seq analysis. Upregulated genes and downregulated genes that were passed through the criteria indicated in Figure S4B are highlighted with light blue dots and dark blue dots, respectively.

(C) Fold change expression of transcription factors in WT1 and Gorlin-1 cells identified as the differentially expressed genes. Fold change expressions of Gorlin-1 cells compared with WT1 cells are shown in log2 ratio.

(D) A list of transcription factors that were upregulated in Gorlin-1 iPSCs compared with WT1 iPSCs and related with bones, mineralization, and osteoblast differentiation in GO analysis.

(E) The mRNA expression of *CDX1*, *FOXO1*, *FOXD1*, and *ID4* in the osteoblast induction culture of WT1, WT2, Gorlin-1, and Gorlin-2 iPSCs. qRT-PCR analysis was performed at day 17 of the culture. Data are the means ± SD from three independent experiments. *$p < 0.05$ versus WT1 iPSCs. **$p < 0.05$ versus both WT1 and WT2 iPSCs.

(F) Calcification in the osteoblast induction culture of WT1 and Gorlin-1 iPSCs with or without GANT61. von Kossa staining was performed at day 17 of the culture.

(G) The mRNA expression of *GLI1*, *CDX1*, *FOXO1*, *FOXD1*, and *ID4* in the osteoblast induction culture of WT1 and Gorlin-1 iPSCs with or without GANT61. qRT-PCR analysis was performed at day 17 of the culture. Data are the means ± SD from three independent experiments. When ANOVA indicated differences among the groups, multiple comparisons among each experimental group were performed using Danette t test. Statistical significance was defined at *$p < 0.05$. Only GLI1 mRNA, the normalized expressions are shown relative to those of WT1 iPSCs on day 17.

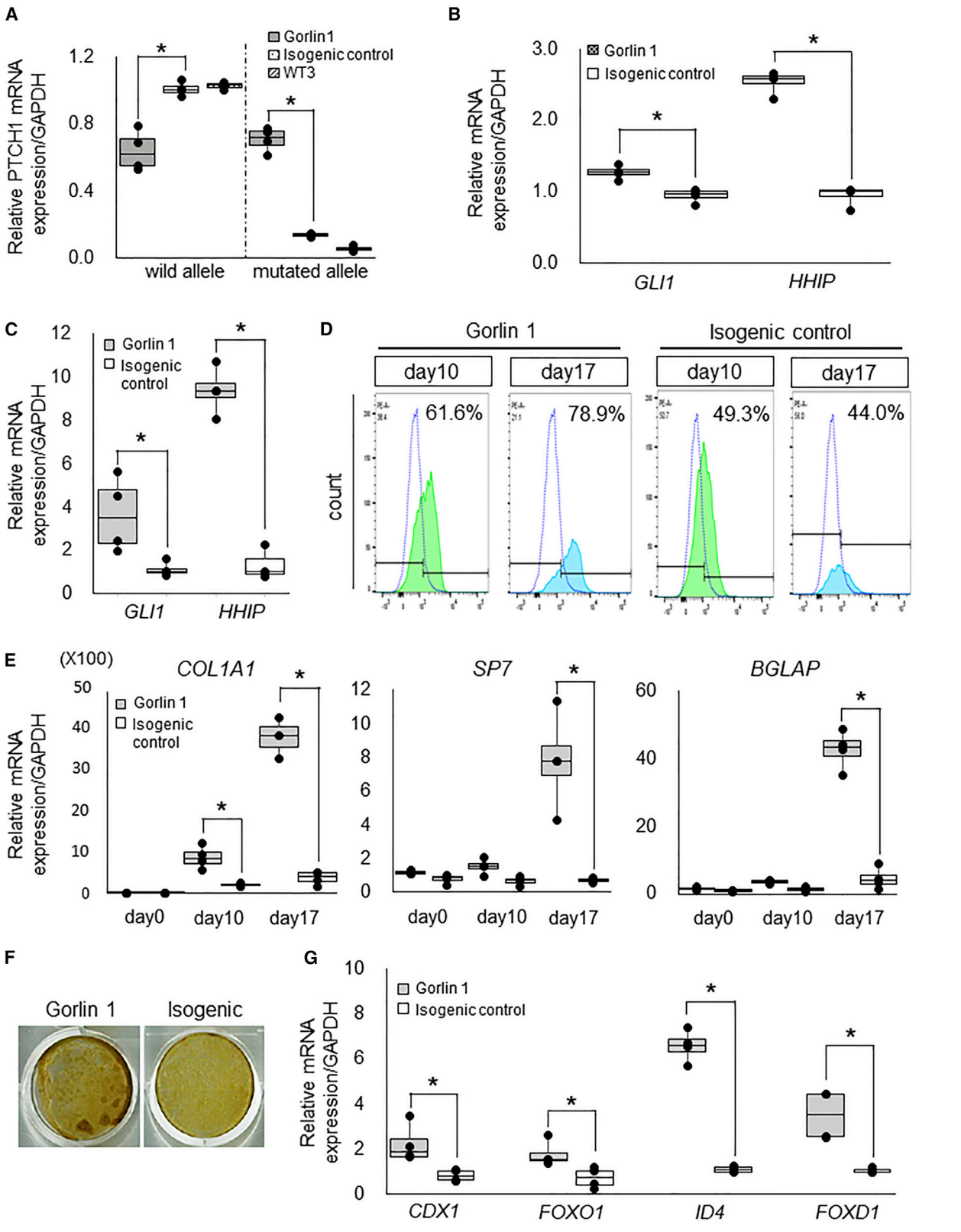


*(legend on next page)*

differentiation rather than proliferation in Gorlin iPSCs under the induction culture.

We next attempted to gain insight into transcriptional networks underlying the positive impacts of *PTCH1* mutation on human osteogenesis. We analyzed differentially expressed TFs between Gorlin and WT iPSCs using PANTHER, a web-based enrichment analysis, and found 14 upregulated and 3 downregulated TFs in Gorlin iPSCs (Figure 3C). Among the 14 upregulated TFs, we selected 4 TFs, *FOXD1*, *ID4*, *FOXO1*, and *CDX1*, because their GO terms were related to bones, mineralization, and osteoblast differentiation (Figure 3D). We also examined these TF expressions in another Gorlin iPSC line (Gorlin 2) derived from a different individual. *FOXO1*, *FOXD1*, and *ID4* were upregulated in both Gorlin-1 and Gorlin-2 iPSCs; however, *CDX1* was not upregulated in Gorlin-2 iPSCs (Figure 3E).

We investigated the involvement of Hh signaling activation in the induction of these TFs in Gorlin iPSCs by treating them with or without GANT61, a direct inhibitor of GLI1. Treatment with GANT61 resulted in neither increase in GLI1 expression nor enhancement of calcification in Gorlin iPSCs at day 17 of the osteoblast induction culture (Figures 3F and 3G). Among the four TFs that we focused on, GANT61 treatment significantly downregulated the expressions of *FOXO1*, *FOXD1*, and *ID4* in Gorlin iPSCs, but not in WT iPSCs, whereas *CDX1* expression was not altered by the treatment in either of the cell lines (Figure 3G), which might reflect the difference in transcriptional networks between different types of *PTCH1* mutations. Overall, these data suggest that *FOXO1*, *FOXD1*, and *ID4* can be targets of canonical Hh signaling (i.e., the Hh-Ptch-Smo-Gli axis) and may underlie the enhancement of osteoblastogenesis and calcification in Gorlin iPSCs. FOXO1 has been reported to provide an intracellular environment congenial to osteoblast differentiation (Kode et al., 2012; Teixeira et al., 2010). CDX1 and FOXD1 take part in development, malignant transformation, and ectopic bone formation coordinately with WNT and BMPs (Regard et al., 2013).

## Comparison of Osteogenic Capacities between Gorlin iPSCs and Their Isogenic Control iPSCs

To eliminate the influence of the different genetic backgrounds of the WT and Gorlin iPSCs, we set out to generate a reliable control iPSC clone for Gorlin-1 iPSCs, in which the mutation in exon 9 (c.1338-1341del CTCA; Figure S5A) was corrected under the same genetic background, i.e., an isogenic control. We utilized a Cas9 nickase-based genome-editing technique in combination with a targeting vector containing a 2-kb homology arm at the 5′ side and a 1.7-kb homology arm at the 3′ side (Figure S5B). We identified five clones showing correct insertion of the pgk-neo cassette (Figure S5C) and selected one clone (clone 9), in which the mutation in the *PTCH1* gene was corrected to the WT sequence, as an isogenic control for Gorlin-1 iPSCs (Figure S5D). The morphology of clone 9 was indistinguishable from that of the original Gorlin-1 iPSCs (Figure S5E). We then checked the WT and mutated *PTCH1* mRNA expression using locked nucleic acid-labeled probes in Gorlin-1 and isogenic control iPSCs. The expression pattern of wild and mutated allele in isogenic control showed similar to another type of control iPSC (WT3). The WT *PTCH1* expression level was lower in Gorlin-1 iPSCs than in the isogenic control, whereas the mutated *PTCH1* level was higher in Gorlin-1 iPSCs (Figure 4A). Gorlin-1 iPSCs showed higher expression levels of *GLI1* and *HHIP* than the isogenic control (Figure 4B).

**Figure 4. Comparison of Osteogenic Capacities between Gorlin iPSCs and Their Isogenic Control iPSCs in the Osteoblast Induction Culture**

(A) The mRNA expression of WT and mutated *PTCH1* alleles under a serum starvation condition (DMEM supplemented with 0.5% fetal bovine serum) in Gorlin-1, their isogenic control iPSCs, and WT3. qRT-PCR analysis was performed at day 2 of the culture. Data are the means ± SD from three independent experiments. *p < 0.05.

(B) The mRNA expression of *GLI1* and *HHIP* under the serum starvation condition in Gorlin-1 and their isogenic control iPSCs. qRT-PCR analysis was performed at day 2 of the culture. Data are the means ± SD from three independent experiments. *p < 0.05.

(C) The mRNA expression of *GLI1* and *HHIP* in the osteoblast induction culture of Gorlin-1 and their isogenic control iPSCs. qRT-PCR analysis was performed at day 17 of the culture. Data are the means ± SD from three independent experiments. *p < 0.05. The normalized expressions are shown relative to those of isogenic control iPSCs on day 17.

(D) Quantification of RUNX2-positive cells in the osteoblast induction culture of Gorlin-1 and their isogenic control iPSCs. FCM analysis was performed for RUNX2 at days 10 and 17 of the culture. Blue dotted lines show signal intensities from the staining with the IgG isotype control. Light blue and green lines show signal intensities from the staining with an anti-RUNX2 antibody.

(E) The mRNA expression of osteoblast marker genes in the osteoblast induction culture of Gorlin-1 and their isogenic control iPSCs. qRT-PCR analysis was performed at the indicated days of the cultures. Data are the means ± SD from three independent experiments. *p < 0.05.

(F) Calcification in the osteoblast induction culture of Gorlin-1 and their isogenic control iPSCs. von Kossa staining was performed at day 17 of the culture.

(G) The mRNA expression of *CDX1*, *FOXO1*, *ID4*, and *FOXD1* in the osteoblast induction culture of Gorin 1 and their isogenic control iPSCs. qRT-PCR analysis was performed at day 17 of the culture. Data are the means ± SD from three independent experiments. *p < 0.05.

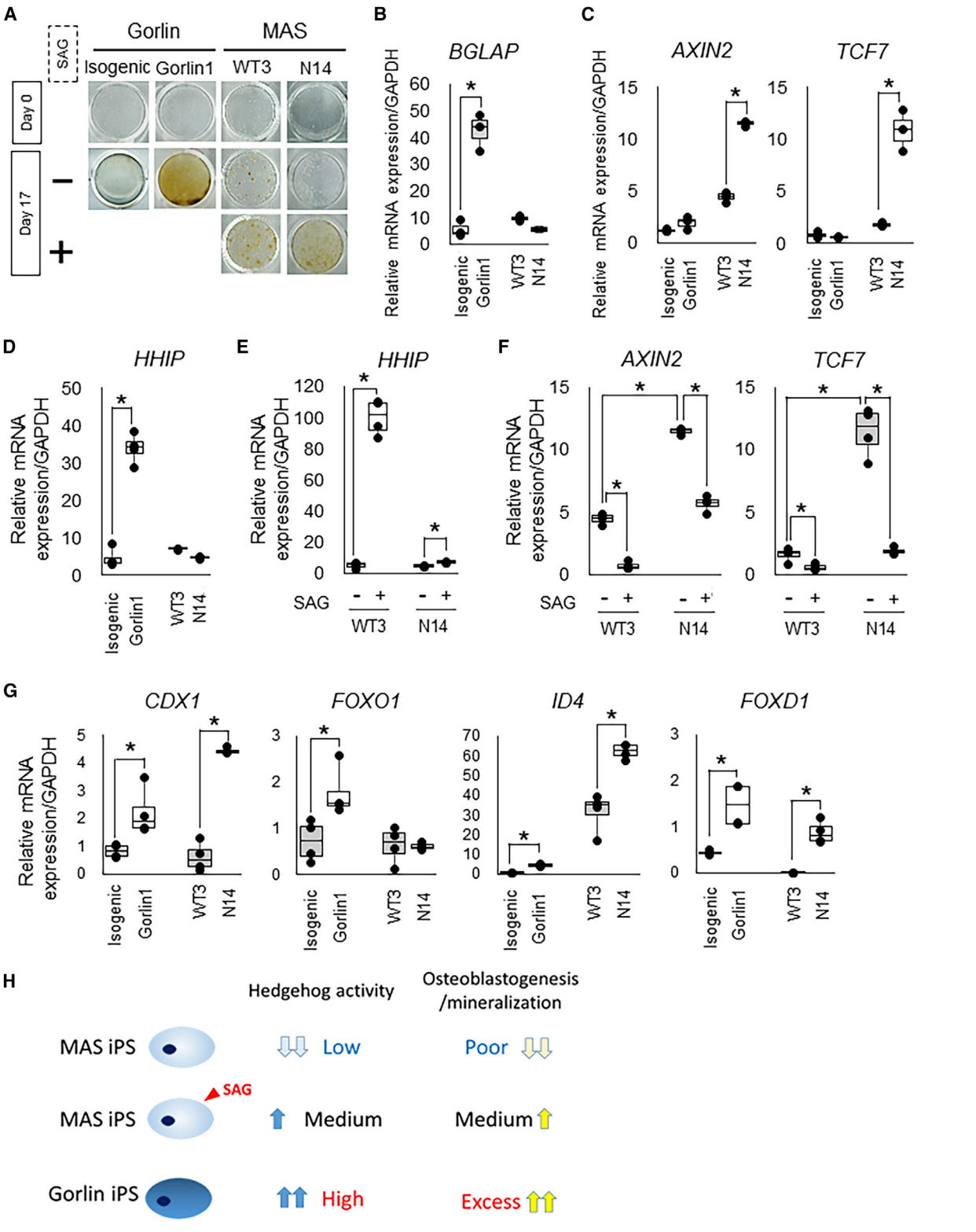


*(legend on next page)*

We compared the osteogenic capacity between Gorlin iPSCs and the isogenic control iPSCs in the osteoblast induction culture. qRT-PCR analysis demonstrated that the expressions of Hh signal-targeting genes, such as *GLI1* and *HHIP* were significantly higher in Gorlin iPSCs than in the isogenic control (Figure 4C). Fluorescence-activated cell sorting analysis at days 10 and 17 showed more RUNX2-positive cells among Gorlin iPSCs than among the isogenic control cells (Figure 4D); expressions of the osteogenic markers *COL1A1*, *SP7*, and *BGLAP* showed significant upregulation only in Gorlin iPSCs at days 10 and 17 (Figure 4E). Gorlin iPSCs demonstrated more calcification than the isogenic control cells at day 17 (Figure 4F). We also compared the expression of the four TFs identified by RNA-seq analysis (Figure 3) between Gorlin iPSCs and the isogenic control iPSCs. All four factors, *CDX1*, *FOXO1*, *ID4*, and *FOXD1*, were upregulated in Gorlin iPSCs compared with the isogenic control cells (Figure 4G). Thus, these findings were consistent with the data obtained from the comparison between Gorlin iPSCs and the irrelevant control iPSCs (Figures 1–3), supporting the positive impact of the Gorlin syndrome-associated *PTCH1* mutation on Hh signaling activity and human osteoblastogenesis, and providing clues to the possible mechanisms underlying the impact.

Given that cyclopamine treatment did not completely repress the mineralization in Gorlin iPSCs (Figure 2D), the enhanced mineralization of Gorlin iPSCs cannot be explained by Hh signaling alone. The four TFs that we found here may also be involved in the phenotype of Gorlin iPSCs. We think that non-canonical Hh pathway and/or other pathways, which are secondarily activated or inhibited, may underlie phenotypes caused by *PTCH1* mutations.

## Hh Signaling Activation Restores the Impaired Osteoblast Formation in *GNAS*-Mutated iPSC-Derived Osteoblasts

In addition to the osteogenic capacities, osteoblastogenesis was prominently enhanced in Gorlin iPSCs. Two genetic diseases associated with osteoblastogenesis, FD and the related disease MAS, have been intensely studied. We recently established an R201H-*GNAS*-mutated iPSC line, N14 (MAS iPSC) by genetic manipulation using a CRISPR/Cas9 system (T.A., S.O., K.W., A.S., T.S. and T.N., unpublished data). In this study, we set out to analyze the calcification of the MAS iPSCs, in addition to Gorlin iPSCs, to gain insight into the involvement of Hh signaling in the mineralization following osteoblastogenesis.

In von Kossa staining, the level of calcification in MAS iPSC-derived cells was much lower than that in control parental iPSCs at day 17 of the osteoblast induction culture (Figure 5A). Although some reports have described that Wnt activation promotes osteoblastogenesis and mineralization (Kato et al., 2002; Rodda and McMahon, 2006), MAS and FD are characterized by poor osteoblastogenesis with immature mineralized bone with high Wnt activity and low Hh activity (Khan et al., 2018). This suggests that

**Figure 5. Hedgehog Activation Rescued a Calcification of GNAS-Mutated MAS iPSC-Derived Osteoblasts**

(A) Calcification in the osteoblast induction culture of Gorlin-1 iPSCs, their isogenic control iPSCs, MAS iPSCs (N14), and their parental cells (WT3) with or without SAG treatment. von Kossa staining was performed at days 0 and 17 of the osteoblast induction culture. Mineral deposition was detected as black staining.

(B) The mRNA expression of *BGLAP* in the osteoblast induction culture of Gorlin-1 iPSCs, their isogenic control iPSCs, MAS iPSCs (N14), and their parental cells (WT3). qRT-PCR analysis was performed at day 17 of the culture. Data are the means ± SD from three independent experiments. *$p < 0.05$.

(C) The mRNA expression of *AXIN2* and *TCF7* in the osteoblast induction culture of Gorlin-1 iPSCs, their isogenic control iPSCs, MAS iPSCs (N14), and their parental cells (WT3). qRT-PCR analysis was performed at day 17 of the culture. Data are the means ± SD from three independent experiments. *$p < 0.05$.

(D) The mRNA expression of *HHIP* in the osteoblast induction culture of Gorlin-1 iPSCs, their isogenic control iPSCs, MAS iPSCs (N14), and their parental cells (WT3). qRT-PCR analysis was performed at day 17 of the culture. Data are the means ± SD from three independent experiments. *$p < 0.05$.

(E) The mRNA expression of *HHIP* in the osteoblast induction culture treated with or without SAG of MAS iPSCs (N14) and their parental cells (WT3). qRT-PCR analysis was performed at day 17 of the culture. Data are the means ± SD from three independent experiments. *$p < 0.05$.

(F) The mRNA expression of *AXIN2* and *TCF7* in the osteoblast induction culture treated with or without SAG of MAS iPSCs (N14) and their parental cells (WT3). qRT-PCR analysis was performed at day 17 of the culture. Data are the means ± SD from three independent experiments. *$p < 0.05$.

(G) The mRNA expression of *CDX1*, *FOXO1*, *ID4*, and *FOXD1* in the osteoblast induction culture of Gorlin-1 iPSCs, their isogenic control iPSCs, MAS iPSCs (N14), and their parental cells (WT3). qRT-PCR analysis was performed at day 17 of the culture. Data are the means ± SD from three independent experiments. *$p < 0.05$.

(H) Schematic illustration of possible molecular mechanisms underlying phenotypes of osteoblasts derived from MAS iPSCs (top), MAS iPSCs with Hh activators (middle), and Gorlin iPSCs (bottom).

Wnt activation does not always correlate with high osteoblastogenesis and mineralization. Rather, we hypothesized that the low Hh signaling activity might be responsible for the poor osteoblastogenesis and immature bone phenotype of MAS or FD. To test this hypothesis, we treated MAS iPSCs with the SAG to upregulate Hh signaling; SAG treatment enhanced mineralization to the same extent not only in the parental cells, but also in MAS iPSC-derived cells (Figure 5A), supporting the above hypothesis. MAS iPSC-derived cells showed a poor response to the osteogenic induction compared with Gorlin iPSCs, as shown by the expression of *BGLAP* (Figure 5B). Regarding the mechanistic aspects of the differential response, MAS iPSC-derived cells showed significant upregulation of the canonical Wnt signaling target genes *AXIN2* and *TCF7* compared with the parental cells in the induction culture, which was consistent with previous findings (Xu et al., 2018), whereas the Gorlin iPSC-derived cells did not (Figure 5C). In contrast, *HHIP*, an Hh signaling target gene, was upregulated in Gorlin iPSC-derived cells, not in MAS iPSC-derived ones (Figure 5D). The SAG treatment, which restored mineralization, upregulated *HHIP* and downregulated *AXIN2* and *TCF7* in MAS iPSC-derived cells (Figures 5E and 5F), suggesting that changes in both Hh and Wnt signaling activities underlie the effect of SAG on osteoblastogenesis.

Next, we investigated the expression levels of the four TFs (*CDX1*, *FOXO1*, *ID4*, and *FOXD1*) that we found in the earlier experiments, to examine whether any common factors acting downstream of Hh signaling underlay the opposite phenotypes of mineralization in Gorlin iPSCs and MAS iPSCs. *CDX1*, *ID4*, and *FOXD1*, but not *FOXO1*, were upregulated in MAS iPSC-derived osteoblasts (Figure 5G); the absence of upregulation of *FOXO1* may be consistent with low Hh activity caused by GNAS activation in MAS iPSCs, suggesting that *FOXO1*, the expression of which may be regulated by Hh signaling activity, commonly underlies the mineralization phenotypes following osteoblastogenesis of MAS iPSCs and Gorlin iPSCs.

## DISCUSSION

Hh signaling is a vital pathway for formation and maintenance of bone tissues. Disruption of Hh signaling virtually disables osteo-chondral tissue formation (Long et al., 2004). In human, *PTHC1* mutations cause constitutive Hh signaling activation and give rise to Gorlin syndrome characterized by neoplastic lesions and skeletal abnormalities (Gorlin, 1995; Gorlin and Goltz, 1960). Gorlin syndrome patients often have hyper-mineralization of bones. In contrast, FD, which has constitutive activation of GNAS with *GNAS* gene mutation (GNAS R201H), often presents poor mineralization. This *GNAS* mutation is also known as a causative mutation of MAS. We generated two of these genetic disease-specific hiPSCs and attempted to elucidate the central roles of Hh in bone pathophysiology. Here, we present three major findings (Figure 5H). First, Gorlin iPSCs showed enhanced mineralization with upregulation of Hh activity and specific TFs (full-length GLI3 and FOXO1). Second, MAS iPSCs showed poor mineralization with reduced Hh activity and no upregulation of *FOXO1* expression; distinctive TFs acting downstream of Hh signaling, particularly *FOXO1*, may commonly underlie the phenotypes of the two diseases. Third, Hh activator SAG treatment normalized premature calcification in MAS iPSCs. These data suggest that Hh signaling may play a central role in osteoblast formation and subsequent bone mineralization, and Hh activator SAG can be an effective therapeutic agent for FD found in solitary FD or MAS.

We found that regulations of GLI3 processing from GLI3FL to GLI3rep mediate the biological outcome of Hh signaling in osteoblasts. The biological function of GLI3 processing has been intensively discussed in mouse limb digit patterning. The ratio of GLI3FL to GLI3rep or their gradient balance was proposed to determine the Shh-mediated numbers and specifications of limb (Wang et al., 2000; Wang et al., 2007; Litingtung et al., 2002). Our data showed that GLI3FL, activator of Hh pathway, was dominant and might further have enhanced Gorlin iPSCs osteoblast differentiation.

A number of studies have shown that the Hh and Wnt signaling pathways are functionally antagonistic (He et al., 2006; Katoh and Katoh, 2006; Xu et al., 1998). Wnt activation was reported to upregulate Gli3, a transcriptional repressor, which in turn suppresses Hh signaling (Alvarez-Medina et al., 2008). In addition, GNAS activates protein kinase A (PKA), and PKA activation promotes GLI3 processing to increase GLI3rep (Orellana and McKnight, 1992; Wen et al., 2010). Based on these findings, we propose the following mechanism to explain the impaired calcification in MAS iPSC-derived osteoblastic cells. The cells with constitutively activated GNAS may have more GLI3 expression due to the activation of Wnt signaling; the increased GLI3 may be progressively processed into GLI3rep by GNAS-mediated PKA activation, causing low Hh signaling activity.

Our results also suggest that *FOXO1* expression may underlie the functional relationship between Hh and Wnt signaling. Mouse models have highlighted profound influences of FoxOs on bone development. Among the four isoforms, *FoxO1* is highly expressed in the skeleton and is also known as a major regulator of osteoblast function and bone metabolism (Ambrogini et al., 2010). *FoxO1*, *3*, and *4* deletion using the *Mx1-cre* driver line (Ambrogini et al., 2010)

and *FoxO1* deletion using the *Col1a1-Cre* driver line (Rached et al., 2010) caused osteoporotic phenotypes in mice. FoxOs promoted maintenance and differentiation of the progenitors into the osteoblast lineage by activation of *Runx2* (Ambrogini et al., 2010; Rached et al., 2010). Consistent with these studies, bone volume and bone formation rate were decreased in *Bglap-Cre*-driven *FoxO1*-deficient mice, which were related to a decreased number of osteoblasts (Zhang et al., 2018). On the other hand, *FoxO1*, *3*, and *4* deletion in *Osterix1* (*Sp7*)-expressing osteoblast progenitors led to high bone mass phenotypes accompanied with increased proliferation of the progenitors in mice; activation of Wnt/β-catenin signaling was observed in the mutants' progenitors (Iyer et al., 2013). These results suggest that FOXOs have diverse functions at different stages of osteoblast differentiation. In addition, a molecular link between FOXOs and Wnt/β-catenin signaling is also reported in colon cancer cell models, in which FOXOs divert β-catenin from TCF- to FOXO-mediated transcription (Hoogeboom et al., 2008).

Previous studies have revealed an association between the activation of canonical Wnt signaling in osteoblasts and increased bone formation (Day and Yang, 2008). It has been reported that deletion of the murine Wnt antagonist, secreted frizzled-related protein 1, increased the trabecular bone mineral density, volume, and mineral apposition rate due to Wnt activation (Bodine et al., 2004). In contrast, our present study and previous reports showed that constitutive activation of GNAS resulted in poor mineralization despite high Wnt activity, indicating that Wnt activation alone is not sufficient for mineralization. Our results further support the idea that activation of Hh signaling at an early stage of osteogenesis is indispensable for subsequent osteoblast maturation and mineralization, and insufficient Hh signaling is likely to be a major cause of the poor bone maturation of FD observed in MAS. The present results also highlight Hh signaling as a potential therapeutic target to promote maturation of MAS osteoblasts (Figure 5H). Thus, this study is an important first step in the consideration of Hh activators as therapeutic agents for the treatment of FD. Our approach may help not only to investigate the pathogenesis of Gorlin syndrome and MAS, but also to understand the molecular mechanisms underlying tissue development and homeostasis, including the essential roles played by Hh in osteoblast maturation and mineralization.

## EXPERIMENTAL PROCEDURES

### Ethics

This study was approved by the ethics committees of Tokyo Dental College (approval no. 533) and the University of Tokyo (approval no. 15-3). Written informed consent was obtained from patients whose cells were isolated and subjected to reprogramming for this study. Data were analyzed anonymously in accordance with the Declaration of Helsinki.

### Osteoblast Differentiation

Osteoblast differentiation of hiPSCs was performed as described previously, with minor modifications (Kanke et al., 2014). B27 + ITS medium was used as the basal medium during the differentiation and was supplemented with small molecules for each step. The B27 + ITS medium consisted of DMEM/F12 (no. 11330-032; Gibco) containing 1× MEM non-essential amino acids (no. 11140-050; Gibco), 1× B-27 serum-free supplement (no. 17504-044; Gibco), 1× ITS + 1 liquid media supplement (no. I2521; Sigma-Aldrich, St. Louis, MO), 0.1 mM 2-mercaptoethanol (no. 21985-023; Gibco), and penicillin/streptomycin (no. P4458; Sigma-Aldrich). After washing the cells with PBS, the 3-day induction protocol was initiated to differentiate the cells toward a mesoderm lineage. In the induction, cells were cultured on vitronectin-coated dishes in B27 + ITS medium supplemented with 20 μM CHIR99021 (no. 4423; Tocris Bioscience, Bristol, UK) and 5 μM cyclopamine (no. C9710; LKT Laboratories, St. Paul, MN). To induce osteoblast differentiation, we then cultured the hiPSC-derived mesodermal cells for 14 days in B27 + ITS medium supplemented with 50 μg/mL ascorbic acid phosphate (no. A4034; Sigma-Aldrich), 10 mM β-glycerophosphate (no. G9422; Sigma-Aldrich), 0.1 μM dexamethasone (no. 041–18861; Wako, Osaka, Japan), and 1 μM of the helioxanthin derivative TH (4-(4-methoxyphenyl)pyrido[4′,3′:4,5]thieno[2,3-b]pyridine-2-carboxamide; synthesized by Tokyo Chemical Industry, Tokyo), in the presence or absence of 1 μM SAG (no. 566660; Merck Millipore, Darmstadt, Germany). The culture medium was replaced daily. For the inhibition of Hh signaling, 0.5 μM cyclopamine was added to the medium.

### Statistical Analysis

All data are expressed as the mean ± SD. When ANOVA indicated differences among the groups, multiple comparisons among each experimental group were performed using Bonferroni's method. Statistical significance was defined at $p < 0.05$.

## DATA AND CODE AVAILABILITY

The RNA-seq data obtained in this work are available at the National Bioscience Database Center (NBDC) hum 0107 (JGAS00000000218).

## SUPPLEMENTAL INFORMATION

Supplemental Information can be found online at https://doi.org/10.1016/j.stemcr.2020.05.008.

## AUTHOR CONTRIBUTIONS

S.Onodera, T.A., and S.Ohba designed the project. S.Onodera, D.H., N.M., K.W., and D.Z. performed the experiments. D.H., N.M., T.N., and T.S. collected data and samples from each patient. S.Onodera., T.A., A.S., T.N., A.Y., U.C., H.H., and S.Ohba analyzed and interpreted the data. S.Onodera, T.A., and S.Ohba wrote the manuscript. T.A. and S.Ohba supervised the project and approved the final version of the manuscript.

## ACKNOWLEDGMENTS

We thank Drs. Mahito Nakanishi (National Institute of Advanced Industrial Science and Technology –AIST), Manami Ohtaka (AIST), and Ken Nishimura (University of Tsukuba) for providing technical assistance. This work utilized the core research facility of the Center for Disease Biology and Integrative Medicine, The University of Tokyo, which was organized by The University of Tokyo Center for NanoBio Integration entrusted by the Ministry of Education, Culture, Sports, Science and Technology (MEXT) Japan. This work was supported by a JSPS KAKENHI grant (no. JP17H04403, no. JP16K20427, and no. JP18H03007); a Rising Star Award Grant from the American Society for Bone and Mineral Research (to S.Ohba); Tokyo Dental College Research Branding Project; the JSPS Graduate Program for Leaders in Life Innovation (GPLLI); the JSPS Core-to-Core Program (Advanced Research Networks); and the Japan Science and Technology Agency (JST) Center of Innovation Program (COI).

Received: January 23, 2020
Revised: May 12, 2020
Accepted: May 13, 2020
Published: June 11, 2020

## REFERENCES

Albright, F., Butler, A.M., Hampton, A.O., Smith, P., Butler, A., Hampton, A., Smith, P., Mastorakos, G., Mitsiades, N., Doufas, A., et al. (1937). Syndrome characterized by osteitis fibrosa disseminata, areas of pigmentation and endocrine dysfunction, with precocious puberty in females. N. Engl. J. Med. *216*, 727–746.

Alman, B.A. (2015). The role of hedgehog signalling in skeletal health and disease. Nat. Rev. Rheumatol. *11*, 552–560.

Alvarez-Medina, R., Cayuso, J., Okubo, T., Takada, S., and Martí, E. (2008). Wnt canonical pathway restricts graded Shh/Gli patterning activity through the regulation of Gli3 expression. Development *135*, 237–247.

Ambrogini, E., Almeida, M., Martin-Millan, M., Paik, J.H., DePinho, R.A., Han, L., Goellner, J., Weinstein, R.S., Jilka, R.L., O'Brien, C.A., et al. (2010). FoxO-mediated defense against oxidative stress in osteoblasts is indispensable for skeletal homeostasis in mice. Cell Metab. *11*, 136–146.

Bodine, P.V.N., Zhao, W., Kharode, Y.P., Bex, F.J., Lambert, A.-J., Goad, M.B., Gaur, T., Stein, G.S., Lian, J.B., and Komm, B.S. (2004). The Wnt antagonist secreted frizzled-related protein-1 is a negative regulator of trabecular bone formation in adult mice. Mol. Endocrinol. *18*, 1222–1237.

Briscoe, J., and Thérond, P.P. (2013). The mechanisms of Hedgehog signalling and its roles in development and disease. Nat. Rev. Mol. Cell Biol. *14*, 416–429.

Day, T.F., and Yang, Y. (2008). Wnt and hedgehog signaling pathways in bone development. J. Bone Joint Surg. Am. *90*, 19–24.

Fujii, K., and Miyashita, T. (2014). Gorlin syndrome (nevoid basal cell carcinoma syndrome): update and literature review. Pediatr. Int. *56*, 667–674.

Goodrich, L.V., Milenković, L., Higgins, K.M., and Scott, M.P. (1997). Altered neural cell fates and medulloblastoma in mouse patched mutants. Science *277*, 1109–1113.

Gorlin, R.J. (1995). Nevoid basal cell carcinoma syndrome. Dermatol. Clin. *13*, 113–125.

Gorlin, R.J., and Goltz, R.W. (1960). Multiple nevoid basal-cell epithelioma, jaw cysts and bifid rib. A syndrome. N. Engl. J. Med. *262*, 908–912.

Hasegawa, D., Ochiai-Shino, H., Onodera, S., Nakamura, T., Saito, A., Onda, T., Watanabe, K., Nishimura, K., Ohtaka, M., Nakanishi, M., et al. (2017). Gorlin syndrome-derived induced pluripotent stem cells are hypersensitive to hedgehog-mediated osteogenic induction. PLoS One *12*, e0186879.

He, J., Sheng, T., Stelter, A.A., Li, C., Zhang, X., Sinha, M., Luxon, B.A., and Xie, J. (2006). Suppressing Wnt signaling by the hedgehog pathway through sFRP-1. J. Biol. Chem. *281*, 35598–35602.

Hoogeboom, D., Essers, M.A.G., Polderman, P.E., Voets, E., Smits, L.M.M., and Burgering, B.M.T. (2008). Interaction of FOXO with β-catenin inhibits β-catenin/T cell factor activity. J. Biol. Chem. *283*, 9224–9230.

Ingham, P.W., and McMahon, A.P. (2001). Hedgehog signaling in animal development: paradigms and principles. Genes Dev. *15*, 3059–3087.

Iyer, S., Ambrogini, E., Bartell, S.M., Han, L., Roberson, P.K., De Cabo, R., Jilka, R.L., Weinstein, R.S., O'Brien, C.A., Manolagas, S.C., et al. (2013). FOXOs attenuate bone formation by suppressing Wnt signaling. J. Clin. Invest. *123*, 3409–3419.

Joeng, K.S., and Long, F. (2009). The Gli2 transcriptional activator is a crucial effector for Ihh signaling in osteoblast development and cartilage vascularization. Development *136*, 4177–4185.

Kanke, K., Masaki, H., Saito, T., Komiyama, Y., Hojo, H., Nakauchi, H., Lichtler, A.C., Takato, T., Chung, U.-I., and Ohba, S. (2014). Stepwise differentiation of pluripotent stem cells into osteoblasts using four small molecules under serum-free and feeder-free conditions. Stem Cell Reports *2*, 751–760.

Kato, M., Patel, M.S., Levasseur, R., Lobov, I., Chang, B.H.-J., Glass, D.A., Hartmann, C., Li, L., Hwang, T.-H., Brayton, C.F., et al. (2002). *Cbfa1*-independent decrease in osteoblast proliferation, osteopenia, and persistent embryonic eye vascularization in mice deficient in Lrp5, a Wnt coreceptor. J. Cell Biol. *157*, 303–314.

Katoh, Y., and Katoh, M. (2006). WNT antagonist, SFRP1, is Hedgehog signaling target. Int. J. Mol. Med. *17*, 171–175.

Khan, S.K., Yadav, P.S., Elliott, G., Hu, D.Z., Xu, R., and Yang, Y. (2018). Induced GnasR201H expression from the endogenous Gnas locus causes fibrous dysplasia by up-regulating Wnt/β-catenin signaling. Proc. Natl. Acad. Sci. U S A *115*, E418–E427.

Kode, A., Mosialou, I., Silva, B.C., Rached, M.-T., Zhou, B., Wang, J., Townes, T.M., Hen, R., DePinho, R.A., Guo, X.E., et al. (2012). FOXO1 orchestrates the bone-suppressing function of gut-derived serotonin. J. Clin. Invest. *122*, 3490–3503.

Komori, T., Yagi, H., Nomura, S., Yamaguchi, A., Sasaki, K., Deguchi, K., Shimizu, Y., Bronson, R.T., Gao, Y.H., Inada, M., et al. (1997). Targeted disruption of Cbfa1 results in a complete lack of bone formation owing to maturational arrest of osteoblasts. Cell *89*, 755–764.

Lichtenstein, L. (1938). Polyostotic fibrous dysplasia. Arch. Surg. *36*, 874.

Litingtung, Y., Dahn, R.D., Li, Y., Fallon, J.F., and Chiang, C. (2002). Shh and Gli3 are dispensable for limb skeleton formation but regulate digit number and identity. Nature *418*, 979–983.

Long, F., Chung, U., Ohba, S., McMahon, J., Kronenberg, H.M., and McMahon, A.P. (2004). Ihh signaling is directly required for the osteoblast lineage in the endochondral skeleton. Development *131*, 1309–1318.

Mullor, J.L., Sánchez, P., and Ruiz i Altaba, A. (2002). Pathways and consequences: hedgehog signaling in human disease. Trends Cell Biol *12*, 562–569.

Ohba, S., Nakajima, K., Komiyama, Y., Kugimiya, F., Igawa, K., Itaka, K., Moro, T., Nakamura, K., Kawaguchi, H., Takato, T., et al. (2007). A novel osteogenic helioxanthin-derivative acts in a BMP-dependent manner. Biochem. Biophys. Res. Commun. *357*, 854–860.

Ohba, S., Kawaguchi, H., Kugimiya, F., Ogasawara, T., Kawamura, N., Saito, T., Ikeda, T., Fujii, K., Miyajima, T., Kuramochi, A., et al. (2008). Patched1 haploinsufficiency increases adult bone mass and modulates Gli3 repressor activity. Dev. Cell *14*, 689–699.

Orellana, S.A., and McKnight, G.S. (1992). Mutations in the catalytic subunit of cAMP-dependent protein kinase result in unregulated biological activity. Proc. Natl. Acad. Sci. U S A *89*, 4726–4730.

Rached, M.-T., Kode, A., Xu, L., Yoshikawa, Y., Paik, J.-H., DePinho, R.A., and Kousteni, S. (2010). FoxO1 is a positive regulator of bone formation by favoring protein synthesis and resistance to oxidative stress in osteoblasts. Cell Metab. *11*, 147–160.

Regard, J.B., Malhotra, D., Gvozdenovic-Jeremic, J., Josey, M., Chen, M., Weinstein, L.S., Lu, J., Shore, E.M., Kaplan, F.S., and Yang, Y. (2013). Activation of Hedgehog signaling by loss of GNAS causes heterotopic ossification. Nat. Med. *19*, 1505–1512.

Rodda, S.J., and McMahon, A.P. (2006). Distinct roles for Hedgehog and canonical Wnt signaling in specification, differentiation and maintenance of osteoblast progenitors. Development *133*, 3231–3244.

St-Jacques, B., Hammerschmidt, M., and McMahon, A.P. (1999). Indian hedgehog signaling regulates proliferation and differentiation of chondrocytes and is essential for bone formation. Genes Dev. *13*, 2072–2086.

Teixeira, C.C., Liu, Y., Thant, L.M., Pang, J., Palmer, G., and Alikhani, M. (2010). Foxo1, a novel regulator of osteoblast differentiation and skeletogenesis. J. Biol. Chem. *285*, 31055–31065.

Turan, S., and Bastepe, M. (2015). GNAS spectrum of disorders. Curr. Osteoporos. Rep. *13*, 146–158.

Wang, B., Fallon, J.F., and Beachy, P.A. (2000). Hedgehog-regulated processing of Gli3 produces an anterior/posterior repressor gradient in the developing vertebrate limb. Cell *100*, 423–434.

Wang, C., Rüther, U., and Wang, B. (2007). The Shh-independent activator function of the full-length Gli3 protein and its role in vertebrate limb digit patterning. Dev. Biol. *305*, 460–469.

Weinstein, L.S., Shenker, A., Gejman, P.V., Merino, M.J., Friedman, E., and Spiegel, A.M. (1991). Activating mutations of the stimulatory G protein in the McCune–Albright syndrome. N. Engl. J. Med. *325*, 1688–1695.

Wen, X., Lai, C.K., Evangelista, M., Hongo, J.-A., de Sauvage, F.J., and Scales, S.J. (2010). Kinetics of hedgehog-dependent full-length Gli3 accumulation in primary cilia and subsequent degradation. Mol. Cell. Biol. *30*, 1910–1922.

Xu, Q., D'Amore, P.A., and Sokol, S.Y. (1998). Functional and biochemical interactions of Wnts with FrzA, a secreted Wnt antagonist. Development *125*, 4767–4776.

Xu, R., Khan, S.K., Zhou, T., Gao, B., Zhou, Y., Zhou, X., and Yang, Y. (2018). Gαs signaling controls intramembranous ossification during cranial bone development by regulating both Hedgehog and Wnt/β-catenin signaling. Bone Res. *6*, 33.

Zhang, Y., Xiong, Y., Zhou, J., Xin, N., Zhu, Z., and Wu, Y. (2018). FoxO1 expression in osteoblasts modulates bone formation through resistance to oxidative stress in mice. Biochem. Biophys. Res. Commun. *503*, 1401–1408.

Zujur, D., Kanke, K., Lichtler, A.C., Hojo, H., Chung, U., and Ohba, S. (2017). Three-dimensional system enabling the maintenance and directed differentiation of pluripotent stem cells under defined conditions. Sci. Adv. *3*, e1602875.